Kinetics of Grain Growth in the Weld Heat-Affected Zone of Alloy 718

B. RADHAKRISHNAN and R.G. THOMPSON

Grain-boundary liquation occurs in the weld heat-affected zone (HAZ) of the Ni-base superalloy 718 at locations where the peak temperatures are greater than about 1200 °C. The evolution of the grain structure at these HAZ locations depends upon the interaction between the grains and the grain-boundary liquid. The evolution of grain structure in the presence of grain-boundary liquid was simulated by subjecting samples to controlled thermal cycles using resistance heating. A measurement of grain size as a function of isothermal hold at two peak temperatures of 1200 °C and 1227 °C indicated that in alloy 718, the kinetics of grain growth depended upon the prior thermal history of the alloy. In the solution-treated alloy, the presence of grain-boundary liquid did not arrest grain growth at either peak temperature. In the homogenized and aged alloy, a grain refinement was observed at the peak temperature of 1227 °C, while an arrest of grain growth was observed at a peak temperature of 1200 °C. Liquid film migration (LFM) and subgrain coalescence, either acting alone or simultaneously, are shown to explain most of the observed microstructural phenomena and the kinetics of grain growth in the alloy.

I. INTRODUCTION

CONSTITUTIONAL liquation of precipitate particles and the subsequent formation of grain-boundary liquid in the subsolidus portion of the weld heat-affected zone (HAZ) have been observed in several commercial alloy.[1–6] The mechanics of transition from the individual pools of liquid, produced by a constitutional liquation of precipitates, to a continuous grain-boundary film involves the capture of the pools of liquid by the moving grain boundaries and the spreading of the liquid along the grain boundaries assisted by surface tension forces.[7] These processes go to completion during the heating cycle and a microstructure consisting of a continuous grain-boundary liquid film is produced at the peak temperature of the thermal cycle, within a certain distance from the fusion line.[7] At HAZ locations where the peak temperatures just exceed the solidus temperature of the matrix, liquation initiates at the grain boundaries independent of the constitutional liquation mechanism to form a continuous film of grain-boundary liquid. Liquation cracks occur in the HAZ if the grain-boundary liquid film remains stable at a temperature and time when the tensile stresses develop in the HAZ close to the fusion zone. Since tensile stresses in the weld HAZ develop only after the HAZ cools down to a certain temperature, the susceptibility to liquation cracking depends on the temperature range during cooling in which the grain-boundary liquid exists.

A predictive model for liquation cracking can be developed if the temporal evolution of the grain-boundary liquid and the thermal stresses can be modeled for any given location in the HAZ. The kinetics of formation and solidification of the grain-boundary liquid in the subsolidus HAZ has been modeled for a simple binary assuming plane-front solidification, local equilibrium at the solid-liquid (S-L) interface, and solute diffusion in the solid.[8] The model also assumed that the grain boundaries were held stationary by the liquid, which completely wet the grain boundaries. Such an assumption was based on the arrest in the grain growth observed for 18Ni maraging steel,[7] where grain-boundary liquid in the subsolidus portion of the HAZ was produced by constitutional liquation of titanium sulfide particles present in the steel.

A. *Liquation and Grain Growth*

The effectiveness of the metastable liquid as an obstacle to grain growth should depend upon the ability of the liquid to wet the grain boundaries, which is a function of the imbalance of the surface tension forces at the triple point between the grain-boundary liquid and the grain boundary. Spreading is favored if the S-L interfacial energy, γ_{sl}, is very small compared to the solid-solid interfacial energy (grain-boundary energy), γ_{ss}. However, since the metastable liquid always reacts with the solid in which it dissolves, in the form of diffusion of solute(s) across the S-L interface, the nonequilibrium S-L interfacial energy is extremely low,[9] and the liquid completely wets the grain boundaries. Hence, it is reasonable to assume that the degree of wetting between the grain boundary and the metastable liquid will be the same for all alloy systems in which a solute in the metastable liquid is soluble in the matrix, irrespective of the fact that the matrix-liquid combinations vary from one alloy system to another. However, since the kinetics of spreading is determined by the diffusion of solute(s) both in the liquid and along the grain boundary,[10] it is expected to vary from one alloy system to another because of differences in solute diffusivity. In any given alloy system, the kinetics of spreading will also depend upon the composition of the grain boundaries, which can be widely varied by prior heat treatments. Equilibrium[11,12]

B. RADHAKRISHNAN, formerly Research Associate, with the Department of Materials Science and Engineering, University of Alabama at Birmingham, Birmingham, AL, is now with the Metals and Ceramics Division, Oak Ridge National Laboratory, TN 37831-6096. R.G. THOMPSON, Professor, is with the Department of Materials Science and Engineering, University of Alabama at Birmingham, Birmingham, AL 35294.

Manuscript received November 18, 1992.

and nonequilibrium[13] segregation processes are known to cause profound alterations to grain-boundary compositions in many alloy systems. The kinetics of spreading can be increased by enriching the grain boundary with respect to alloying elements which partition to the liquid.

In some alloy systems, the presence of a metastable liquid film along the grain boundaries causes a chemically induced migration of the boundaries.[14,15] Hence, the liquid film does not effectively pin the grain boundaries in these alloys. The phenomenon, known as liquid film migration (LFM), is caused by the presence of a coherency strain in the matrix at the matrix-liquid interface.[16] The migration can occur at both subsolidus and supersolidus temperatures. At subsolidus temperatures, the coherency strain is produced by the backdiffusion of solute from the solute-rich liquid into the matrix. At supersolidus temperatures, coherency strain is produced by the formation of a solute-depleted matrix at the matrix-liquid interface by the melting of the grain-boundary regions.

Hence, it appears that the obstacle to HAZ grain growth by metastable liquid is a complex function of several microstructural variables which vary not only from one alloy system to another, but also within an alloy system.

B. *HAZ Liquation in Alloy 718*

In alloy 718, the formation of grain-boundary liquid in the subsolidus HAZ may be due to the constitutional liquation of carbides,[17] Laves,[18,19,20] silicides,[20] and borides.[20,21] The primary mechanism for the formation of grain-boundary liquid in wrought alloys was considered to be the constitutional liquation of carbides,[22] since Laves phase is metastable and can be dissolved during heat treatment, and since the volume fraction of minority phases such as borides and silicides are extremely small in wrought alloy 718 of nominal composition. The evolution of a diffusion couple between NbC and γ matrix of alloy 718 at temperatures above the pseudoternary eutectic temperature of the alloy was shown to result in the formation of metastable liquid.[22]

In order to provide a basic understanding of grain-boundary liquation in alloy 718, isothermal liquation studies[23] were undertaken, using an approach similar to that of Pepe and Savage.[7] The results indicated several interesting deviations from the constitutional liquation behavior of titanium sulfide inclusions in 18Ni maraging steel. A time delay was associated with the formation of metastable liquid by the constitutional liquation of carbides. This delay in carbide liquation was present for the solution-treated as well as the aged alloys in the subsolidus portion of the HAZ where the peak temperatures were just above the carbide liquation temperature.[23] However, for the aged alloy, there was an instantaneous formation of grain-boundary liquation which preceded the carbide liquation. This difference in the liquation kinetics in the subsolidus portion of the HAZ was proposed to be one of the reasons for the heat-treatment dependent variations in the liquation cracking susceptibility of alloy 718.[23]

Isothermal liquation studies also indicated the occurrence of migration of the liquated grain boundaries,[24] which showed that the grain boundaries were not effectively pinned by the liquid, as observed in 18Ni maraging steel.[7] The present study is a continuation of earlier work on isothermal liquation kinetics in alloy 718[23] which attempts to highlight the interaction between liquation and grain size in the HAZ of alloy 718. The ultimate objective of the isothermal liquation studies[23] was to provide a basic understanding of the interactions between HAZ thermal cycle, initial microstructure, liquation kinetics, and grain growth in alloy 718, which will provide inputs to a more realistic physical modeling of the solidification of grain-boundary liquid in alloy 718.

II. EXPERIMENTAL PROCEDURE

The composition of the alloy 718 used in this study is shown in Table I. A detailed description of the Gleeble thermomechanical device and the experimental procedure used for thermal simulation are available elsewhere[23] and will not be repeated here. Table II provides a description of the various initial heat treatments received by the alloy prior to HAZ thermal simulation. Table III gives a summary of the isothermal liquation studies carried out in the Gleeble. The samples were heated to the peak temperatures in about 8 seconds, held for the various time intervals, and quenched to room temperature in a jet of water.

After thermal cycling, the samples were sectioned transversely at the midpoint of the gage length and the transverse sections were mounted and polished using standard metallographic techniques and etched electrolytically in 10 pct oxalic acid at 5 volts for 5 seconds. The transverse sections were taken within 0.5 mm from the spot where the thermocouple leads were initially welded so that variations due to longitudinal temperature gradients were eliminated.

Optical microscopy was carried out in a Zeiss metallograph using interference contrast. Scanning electron microscopy (SEM) was carried out using a Phillips 515 SEM at an operating voltage of 30 KV. Grain size measurements were made in the Zeiss metallograph by counting N_L, the number of intercepts of the grain boundary per unit length of a test-line placed randomly. The grain size was measured as $1/N_L$. For each sample, counts were made at a constant radial distance of 0.5 mm from the periphery in order to eliminate variations due to radial temperature gradient. About 40 to 50 placements were made for each sample around the periphery, and the average N_L value was used for grain size calculations. The grain growth kinetics at the respective peak temperatures was represented by a plot of

Table I. Composition of Alloy 718

Element	Wt Pct	Element	Wt Pct
Cr	18.12	Si	0.11
Fe	19.07	Ti	0.94
Ni	53.24	B	0.003
Nb + Ta	5	C	0.03
Mo	2.28	S	0.001
Al	0.52	Co	0.09

Table II. Summary of Heat Treatments

Heat Treatment	Description
As-received	Solution treated according to AMS 5662.
Homogenized	Rapidly heated to 1093 °C in about 8 s in the Gleeble, held for 100 s and quenched to room temperature.
Homogenized and aged (A)	1093 °C for 5 min, air-cooled to room temperature, 650 °C for 120 min.
Homogenized and aged (B)	1093 °C for 1 h, air-cooled to room temperature, 650 °C for 10 h.

Table III. Summary of Isothermal Liquation Studies

Heat Treatment	Gleeble Thermal Cycle
As-received	Heat to 1200 °C and 1227 °C in about 8 s, hold isothermally for 0 to 13 s at each temperature and water-quenched to room temperature.
Homogenized	Heat to 1235 °C in about 8 s and water-quench to room temperature.
Homogenized and aged (A)	Heat to 1200 °C in about 8 s, hold isothermally for 0 to 13 s and water-quench to room temperature.
Homogenized and aged (B)	Heat to 1227 °C in about 8 s, hold isothermally for 0 to 8.4 s and water-quench to room temperature.

D vs t, where *D* was the grain size after an isothermal hold of *t* seconds at the peak temperature.

III. RESULTS

The microstructures of the as-received alloy are shown in Figure 1. The as-received alloy had a grain size of ASTM 10, with plates and spheroids of $Ni_3Nb(\delta)$ precipitated both in the matrix and along grain boundaries. The microstructures after the homogenization heat treatments are shown in Figure 2. Following the dissolution of the δ, some of the grain boundaries appear to be missing, as shown in Figure 2.

A. *Liquation Microstructures*

1. *As-received alloy*

Figures 3 and 4 show the progression of grain growth in the as-received alloy as a function of isothermal hold

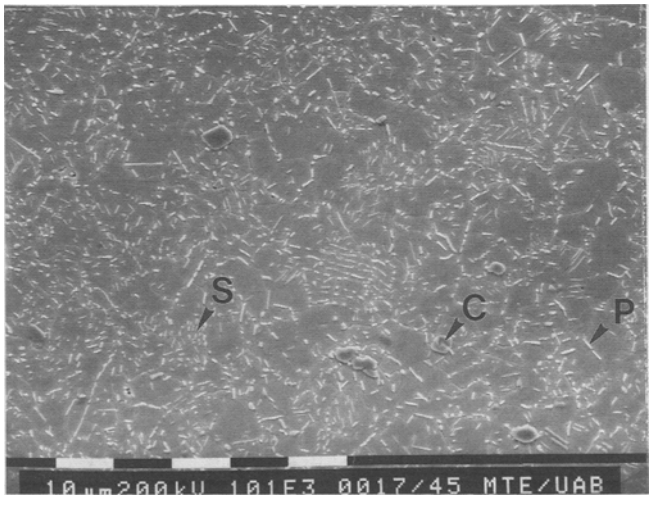

Fig. 1—Microstructure of the as-received alloy showing the carbides (C) and (δ) with platelike (P) and spherodized (S) morphologies.

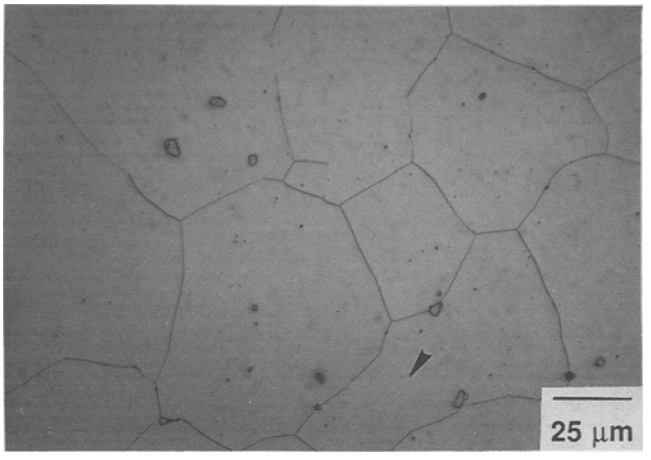

(*a*)

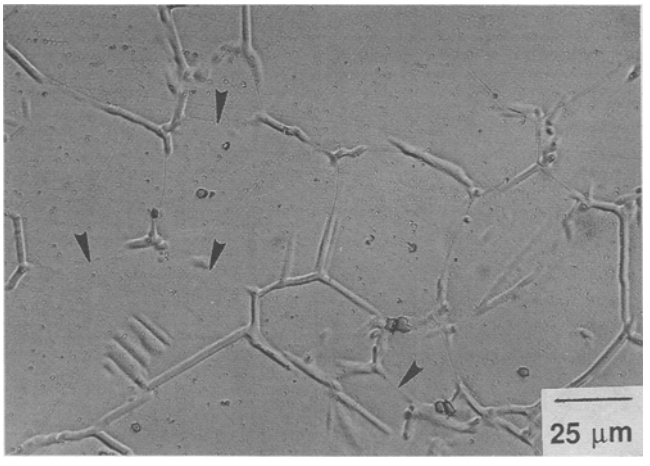

(*b*)

Fig. 2—Microstructures of the as-received alloy after (*a*) homogenization at 1093 °C for 5 min followed by aging at 650 °C for 120 min (heat treatment A) and (*b*) homogenization in the Gleeble at 1093 °C for 100 s. The grain boundaries appear to be missing at the locations marked by arrows.

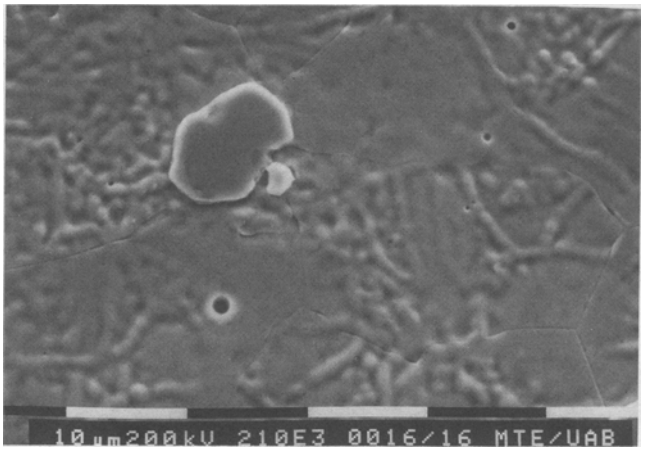

(*a*)

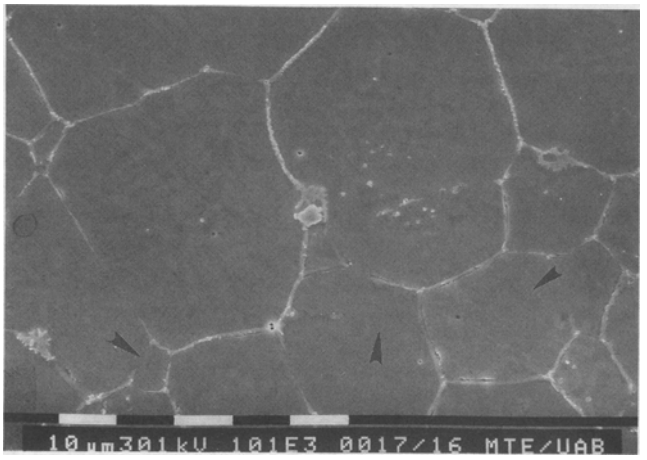

(*b*)

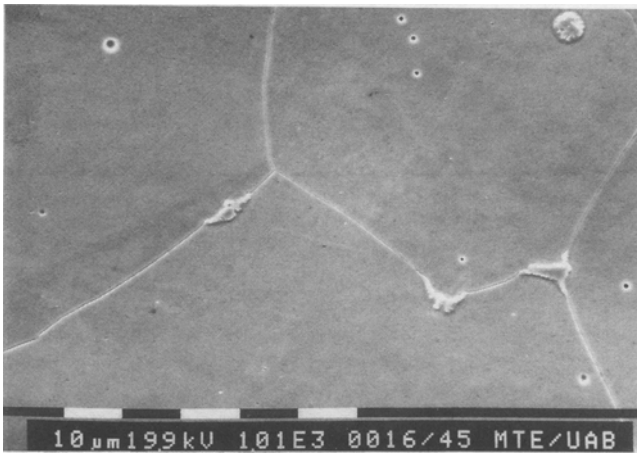

(*c*)

Fig. 3—Microstructure of the as-received alloy heated to a peak temperature of 1200 °C and quenched after an isothermal hold of (*a*) 0.4 s, (*b*) 3.6 s, and (*c*) 13 s. Notice the disappearance of grain boundaries is indicated in (b) at the locations marked by arrows.

at peak temperatures of 1200 °C and 1227 °C, respectively. After an isothermal hold of 1.4 seconds at 1200 °C (Figure 3(a)), the homogenization of the matrix was not yet complete following the dissolution of δ. The grain boundaries were barely discernible and the carbides had not yet liquated. A careful observation of Figure 3(a) shows the ghost image of the original grain-boundary network superimposed on the existing network. A comparison of the two networks shows that the grains had grown appreciably as compared to the as-received alloy. Figure 3(b) shows carbide liquation and the formation of grain-boundary liquid at this temperature after an isothermal hold of about 3 to 4 seconds. The presence of grain-boundary liquid does not appear to arrest grain growth at this temperature. Continued grain growth in the presence of grain-boundary liquid appeared to occur by the sudden disappearance of certain boundaries. Absence of grain boundaries can be seen in the areas marked by arrows in Figure 3(b). The grain-boundary liquid produced at this peak temperature is seen to disappear completely upon continued isothermal holding, indicating the metastable nature of the liquid.

At a peak temperature of 1227 °C, the liquation of carbides and Nb-rich areas produced by the dissolution of δ occurred almost instantaneously upon reaching the peak temperature, as shown in Figure 4. Figures 4(a) through (d) show several interesting microstructural features. Quadruple points (Q) were seen in several locations in Figure 4(a). The grain boundaries appeared tortuous. Figure 4(b) shows circular grains in several locations. Pools of liquid (P) appeared to collect at the triple and quadruple points as shown in Figures 4(c) and (d). These microstructural features will be shown to be caused by the occurrence of liquid film migration (LFM)[24] in the alloy.

The extent of intragranular liquation in Figure 4 appeared to decrease as a result of the isothermal hold. Figure 5 shows the mechanism of formation of the intragranular specks of liquid seen in Figures 4(a) through (d). The SEM microstructure shows an area where the streaks of liquid (B) break up and form several droplets (C).

2. *Homogenized and aged alloys*

The microstructures of the homogenized and aged alloy (A) heated to a peak temperature of 1200 °C and held isothermally for different time periods are shown in Figure 6. Notice that there was a delay in the liquation of the carbides, similar to the one noticed for the as-received alloy shown in Figure 3. However, there was an instantaneous grain-boundary reaction upon reaching the peak temperature which caused some of the grain boundaries to etch darker. Also, there was an evidence of LFM[10] in these grain boundaries, which showed that the instantaneous reaction was indeed associated with grain-boundary liquation.

Figure 7 shows the microstructure of the homogenized and aged alloy (B) heated to a peak temperature of 1227 °C and held isothermally. Notice that migration of the liquated boundaries resulted in the formation of tortuous grain boundaries and also the formation of several small grains at the original grain boundaries. It was shown[24] in an earlier article that migration at a peak

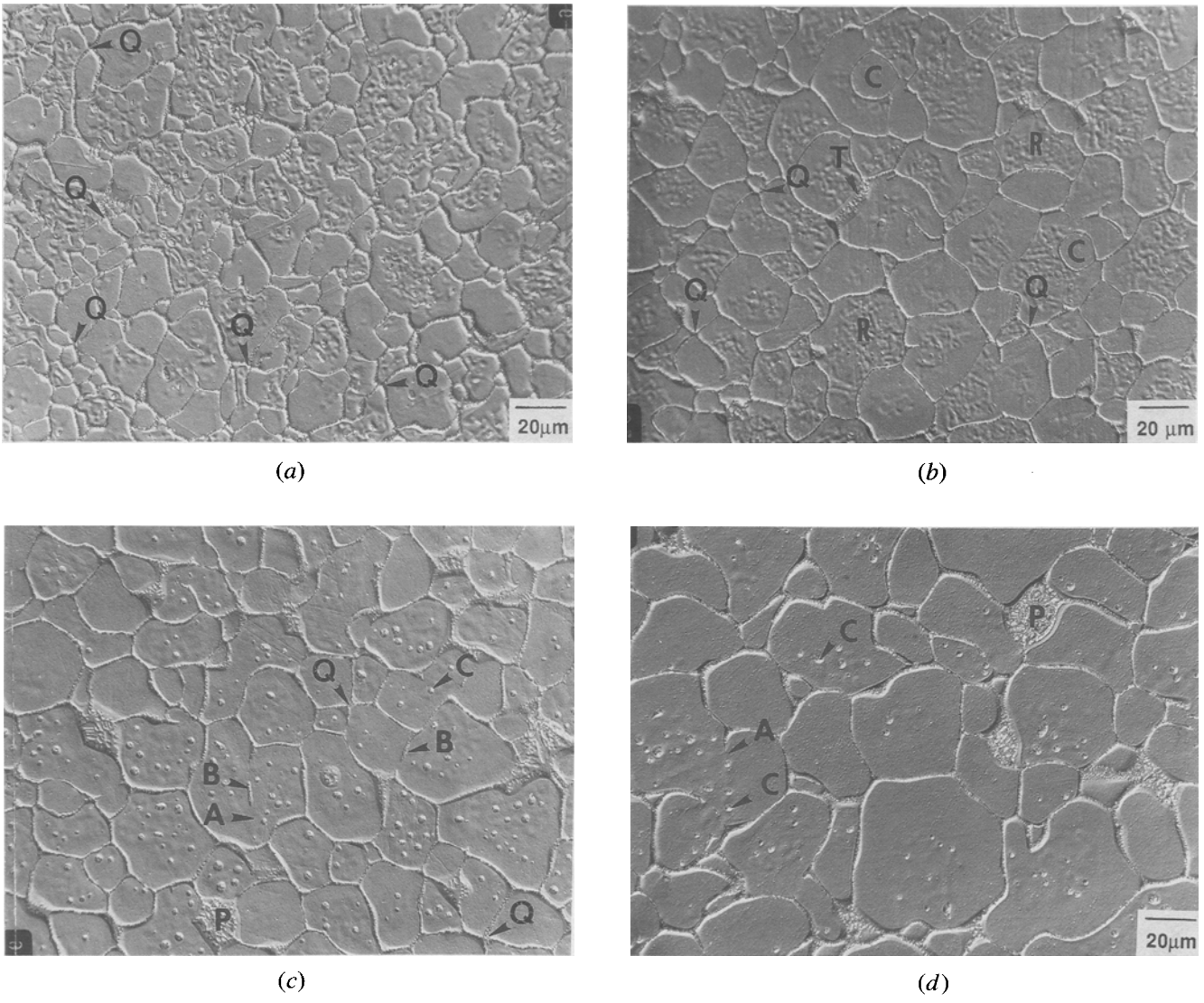

Fig. 4—Microstructure of the as-received alloy heated to a peak temperature of 1227 °C and quenched after an isothermal hold of (*a*) 0.4 s, (*b*) 1.4 s, (*c*) 6 s, and (*d*) 18 s. Notice the formation of several quadruple points (Q), and circular grains (C) which are free from the surface relief effects (R) seen in some of the grains. The grain boundary marked T in (b) has a thicker film of liquid than the adjacent boundaries. Notice the formation of patches of liquid (P) at the triple points, the absence of grain boundaries in the places marked "A," and the subsequent formation of intragranular streaks (B) and specks (C) of liquid in (c) and (d).

temperature of 1200 °C was associated with niobium enrichment. However, migration at a peak temperature of 1227 °C did not show such a niobium enrichment as shown in Figure 8. In fact, it appears that there is niobium depletion behind the migrating boundaries.

3. *Homogenized alloy*

Figure 9 shows the liquation microstructures at various longitudinal locations of the Gleeble sample subjected to the *in situ* homogenization treatment shown in Table II and subsequently heated to a peak temperature of 1235 °C at the center of the gage length. Notice the reduction in grain size as the peak temperature was progressively increased.

B. *Kinetics of Grain-Boundary Motion*

The kinetics of grain growth for the as-received and heat-treated alloys at peak temperatures of 1200 °C and 1227 °C are shown in Figure 10. The measurement of grain size at 1227 °C posed some experimental difficulties due to the presence of intragranular films in several areas, which could not be distinguished from grain-boundary liquid. However, the N_L measurements included all the intercepts of the liquated films with the test-lines, except those isolated specks and streaks of liquated regions which could be clearly distinguished as intragranular liquation.

Notice that the formation of grain-boundary liquid in the as-received alloy both at 1200 °C and at 1227 °C did not arrest grain growth in the alloy, although the formation of the transient metastable liquid at 1200 °C appeared to momentarily retard the grain-growth kinetics. At a peak temperature of 1227 °C where the volume fraction of grain-boundary liquid was greater, the kinetics of grain growth was lower than that at 1200 °C. Figure 11 shows a plot of $(D^3 - D_0^3)$ *vs* (t) for the grain

growth data at 1227 °C. The significance of this plot will be discussed later. After an isothermal hold of about 13 seconds, the grain size appeared to stabilize at both of the peak temperatures. However, the grain size at 1200 °C appears to stabilize at a greater value than at 1227 °C. In the case of the homogenized and aged alloy (A), the instantaneous liquation of the grain boundaries and the delayed liquation of the carbides both resulted in a pronounced arrest of grain-boundary motion. The isothermal grain growth kinetics of the aged alloy (B) at a peak temperature of 1227 °C is shown in Figure 12. Notice that the grain size, as measured by the intercept method, decreases as a function of isothermal hold at this temperature. Figure 13 shows the volume fraction of the total liquid in the as-received alloy as a function of isothermal hold at a peak temperature of 1227 °C. Notice that the initial volume fraction of liquid decreased as a result of isothermal hold.

IV. DISCUSSION

There is a significant difference between the results presented in this study and those of Pepe and Savage,[7] on the effect of grain-boundary liquation on HAZ grain-growth kinetics. While the liquid produced by the constitutional liquation of titanium sulfide inclusions completely arrested grain growth in 18Ni maraging steel, the mobility of the liquated grain boundaries in alloy 718 as determined by grain-growth kinetics appeared to depend upon the thermal history of the alloy prior to HAZ thermal cycling (Figures 10 and 11). A complete arrest of grain-boundary motion was observed in the subsolidus HAZ (1200 °C) of the homogenized and aged alloy in the presence of an instantaneous grain-boundary liquation which preceded the carbide liquation. The delayed subsolidus liquation of carbides was apparently unaccompanied by a pronounced arrest of grain growth in the as-received alloy. There was considerable grain-boundary motion in both the as-received alloy and the homogenized and aged alloy at a peak temperature of 1227 °C. While there was a grain growth in the as-received alloy, there was a grain refinement in the homogenized and aged alloy at this peak temperature. Following is a theoretical explanation which attempts to explain the observed grain-growth behavior in the HAZ of alloy 718.

A. *As-received Alloy*

1. *Grain growth at 1200 °C*

The limiting grain size at a given temperature is determined by the volume fraction of precipitate particles pinning the grain boundaries.[25] The initial grain size in the as-received alloy is stabilized by the volume fractions of NbC and δ in the microstructure. However, during rapid heating, the δ precipitates are known to dissolve at a peak temperature of about 1010 °C.[26] The dissolution of δ precipitates during heating can be seen by the accompanying surface relief (R) shown in Figure 3. However, the local solidus of the solute-rich matrix regions resulting from the δ dissolution is greater than 1200 °C,[22] and hence, these regions do not undergo constitutional liquation. Hence, at the peak temperature a sudden unpinning of the grains occurs, which results

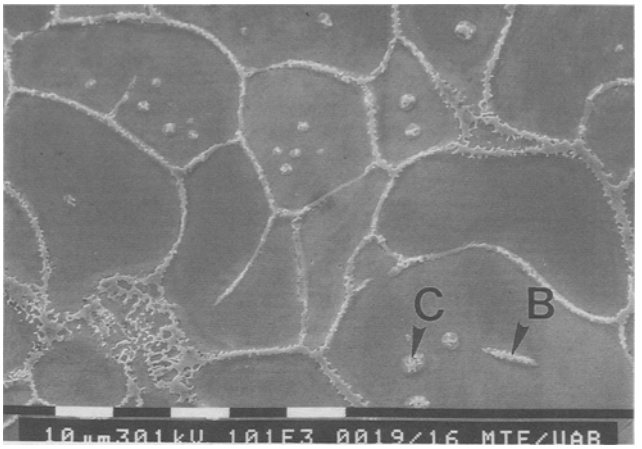

(*a*)

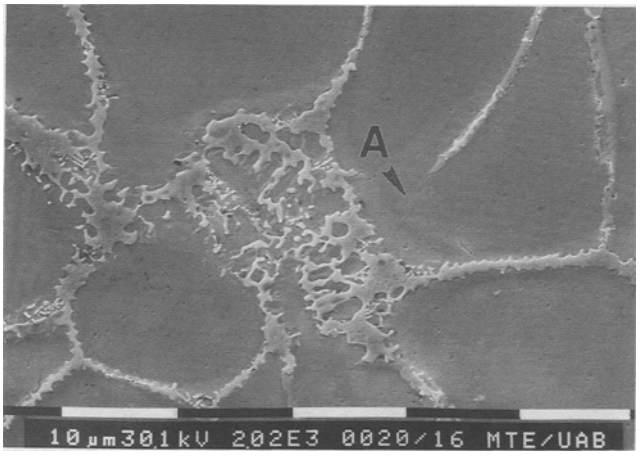

(*b*)

Fig. 5—Microstructure of the as-received alloy heated to a peak temperature of 1227 °C and quenched after an isothermal hold of 18 s. (*a*) The grain-boundary liquid seems to disappear in the areas marked "A." In the region marked "B," there is a streak of intragranular liquid. Areas like these become the intragranular spots of liquid marked "C." (*b*) Region "A" in (a) shown at a higher magnification, indicating the absence of grain boundary at "A."

in grain growth. The kinetics of grain growth in the presence of precipitates has been modeled by Srolovitz *et al.*[27] It was shown that when an initial grain configuration, stabilized by a certain volume fraction of obstacles, is made unstable by a sudden random reduction of the obstacles, grain growth occurs. The grain size stabilizes to a limiting value, which is governed by the reduced volume fraction of the obstacles. In the present study, the limiting grain size at 1200 °C is governed by the volume fraction of carbides at the peak temperature. The grain size appears to be reaching such a limiting value after the initial explosive grain growth at a peak temperature of 1200 °C.

However, such a transient grain growth should be curvature-driven and, hence, should satisfy the well-known kinetic equation[25]

$$D^m - D_0^m = kt \qquad [1]$$

where D is the grain size after an isothermal hold of t

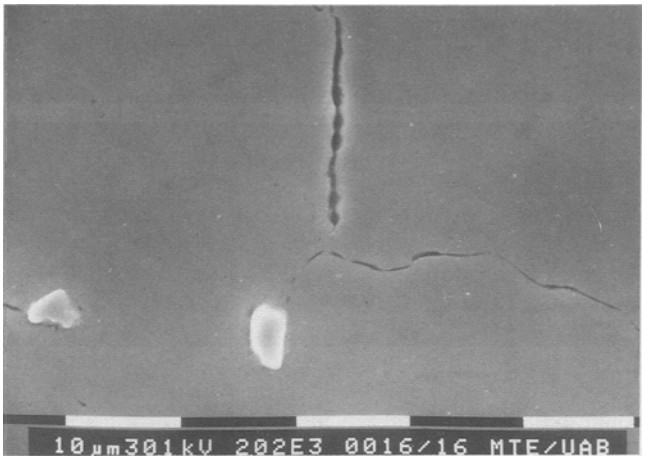

(*a*)

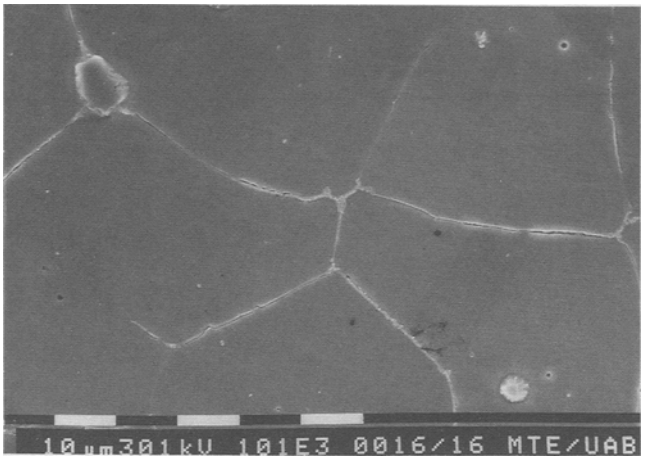

(*b*)

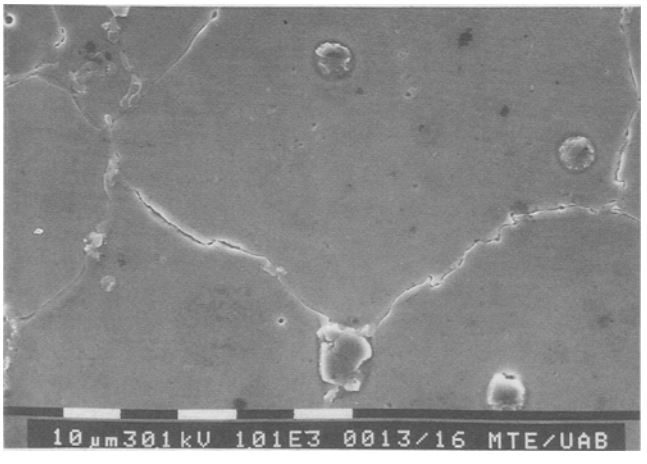

(*c*)

Fig. 6—Microstructure of the homogenized and aged alloy (heat treatment A) heated to a peak temperature of 1200 °C and quenched after an isothermal hold of (*a*) 0.4 s, (*b*) 6.2 s, and (*c*) 13 s.

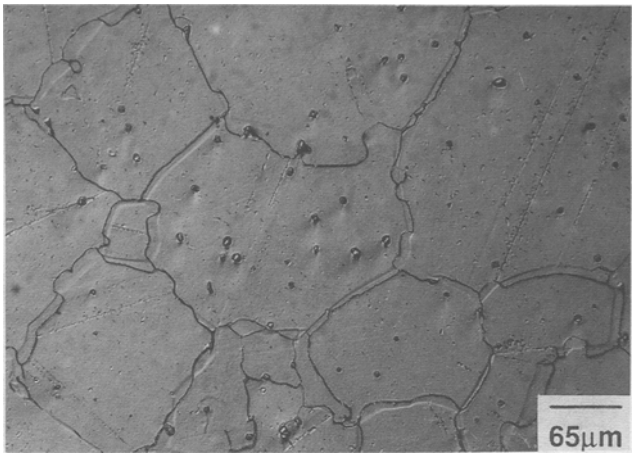

(*a*)

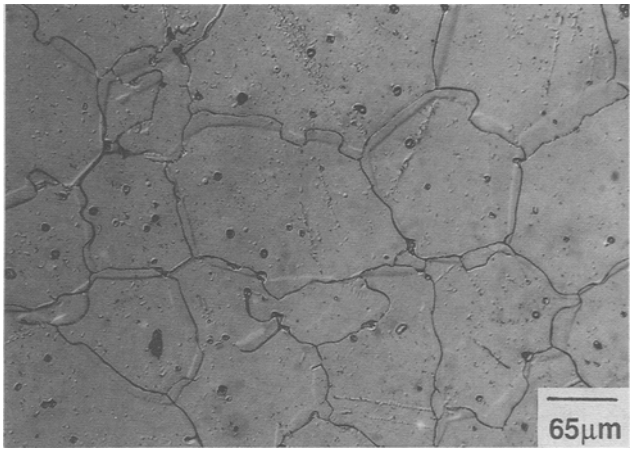

(*b*)

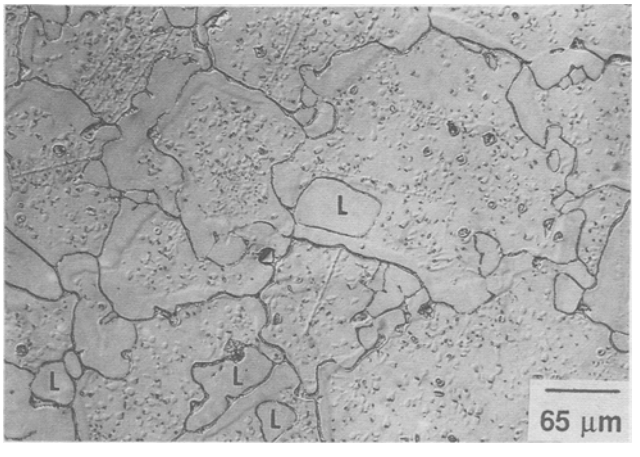

(*c*)

Fig. 7—Microstructure of the homogenized and aged alloy (heat treatment B) heated to a peak temperature of 1227 °C and quenched after an isothermal hold of (*a*) 1.4 s, (*b*) 3 s, and (*c*) 8.2 s.[24] LFM results in grain boundaries becoming tortuous and also the formation of several small grains (L) at the original grain boundaries.

Fig. 8—BSE image of one of the migrating grain boundaries shown in Figure 9. Notice the lack of Nb enrichment behind the migrating boundaries.

seconds, D_0 is the grain size at $t = 0$, and k is a temperature-dependent rate coefficient. For curvature-driven grain growth, m generally ranges from 2 to 6, depending upon the temperature and the purity of the alloy. By differentiating Eq. [1] with respect to time,

$$\frac{dD}{dt} = k'D^{1-m} \qquad [2]$$

where $k' = k/m$. For values of m ranging from 2 to 6, or for any other value greater than 1, the slope of the grain-growth curve should monotonously decrease with grain size.

From Figure 10, it can be seen that the grain-growth data for the as-received alloy at a temperature of 1200 °C cannot be explained on the basis of curvature-driven growth, since the slope of the grain-growth curve does not decrease monotonically with time. However, a sudden increase in the growth rate is seen clearly after an isothermal hold of 3 to 4 seconds, indicating a change in the dominant grain-growth mechanism.

The thermomechanical history of the as-received alloy was not precisely known. However, it is known[28] that during the thermomechanical processing of alloy 718, the final hot-working temperature is below the δ solvus temperature. The presence of δ phase during hot-working prevents the growth of recrystallized grains.[28] Although a TEM investigation of the as-received microstructure was not undertaken in the present study, such an observation of an alloy 718[29] subjected to an identical thermal history (forging below δ solvus, followed by solution anneal below δ solvus) was known to result in a partially recrystallized microstructure, which consisted of spheroidized δ precipitates in the recrystallized grains and platelike δ precipitates in the unrecrystallized grains.[29] It is possible that a similar microstructure consisting of both recrystallized grains and polygonized subgrains stabilized by δ precipitates was obtained in the as-received alloy of the present study. Notice that the as-received microstructure (Figure 1) shows both the platelike and spheroidized δ morphologies.

The grain boundaries in the as-received material could not be distinguished clearly. This could be due to the presence of a large number of subgrains and the large volume fraction of δ phase precipitated along the subgrain boundaries. However, from an examination of the ghost-boundary network in Figure 3(a), the initial grain size can be estimated to be about 10 μ. The grain boundaries could be seen clearly only in samples isothermally held for 1.4 seconds at 1200 °C. By this time the grains had grown from about 10 μ in the as-received material to about 20 μ in the sample heated to 1200 °C, indicating a very rapid growth rate. This growth could have occurred only after heating above about 1000 °C, when the δ phase started to dissolve. It is possible that this initial grain rapid growth was due to the release of the stored

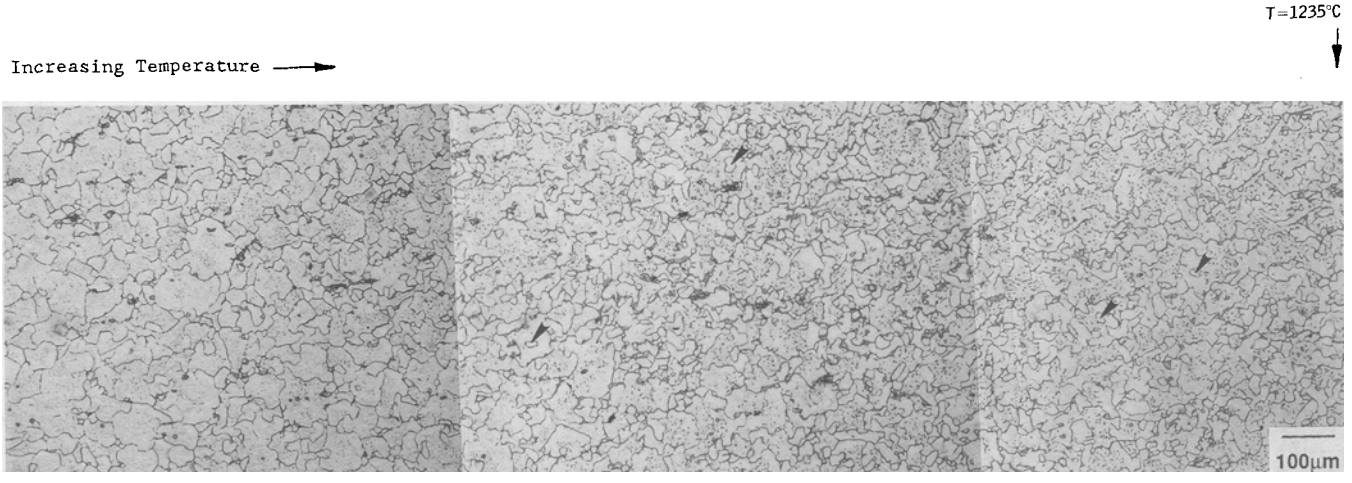

Fig. 9—Liquation microstructures at various longitudinal locations of a Gleeble sample heated to a peak temperature of 1235 °C at the center. The sample was subjected to a homogenization heat treatment in the Gleeble at 1093 °C for 100 s, prior to heating to 1235 °C. The extreme right corresponds to a peak temperature of 1235 °C. The peak temperature progressively decreases from right to left. Notice the increasing extent of LFM from right to left and the corresponding decrease in the grain size. Loops of liquated areas (indicated by arrows) are similar to those seen in Figure 7(c).

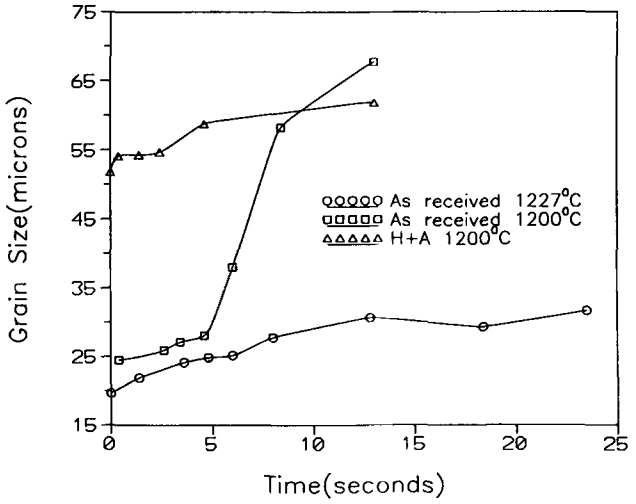

Fig. 10—Kinetics of grain growth for the as-received and the homogenized and aged alloy (heat treatment A) at peak temperatures of 1200 °C and 1227 °C.

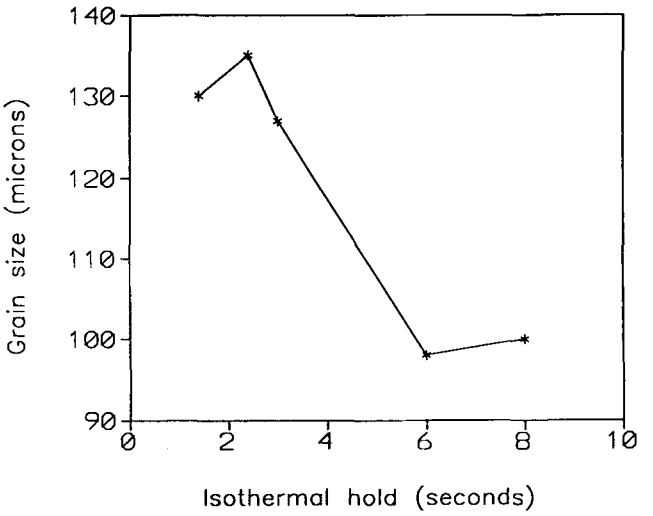

Fig. 12—Variation of grain size with isothermal hold at 1227 °C for the homogenized and aged alloy (heat treatment B).

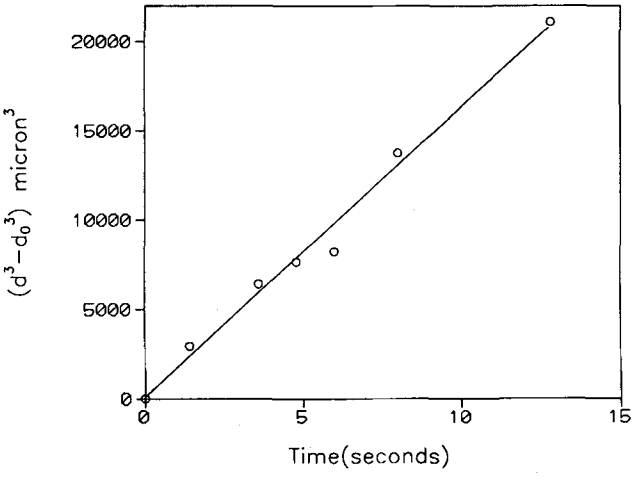

Fig. 11—Plot of $(d^3 - d_0^3)$ *vs* time for the grain growth data at 1227 °C for the as-received alloy. The best-fit straight line passes through the origin.

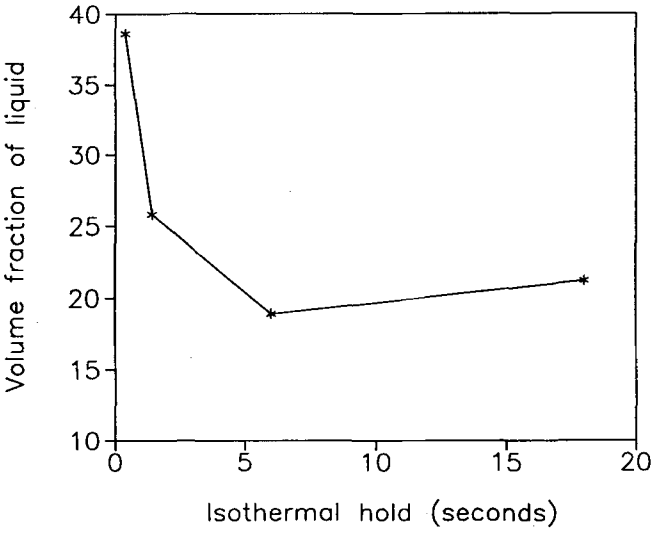

Fig. 13—Volume fraction of liquid as a function of isothermal hold at 1227 °C for the as-received alloy.

energy of deformation which was apparently not completely removed during the hot-working process in the presence of the δ phase in the microstructure. Following an isothermal hold of about 3 to 4 seconds, there was again a rapid increase in the growth rate. Careful investigation of microstructures of these samples indicated that the rapid grain growth could have resulted from the sudden disappearance of some of the boundaries. The disappearance of some of the boundaries is shown in Figure 3(b).

The disappearance of grain boundaries appeared similar to the subgrain coalescence mechanism reported in the literature by Li[30] for grain growth following polygonization, where the subgrains were supposed to rotate in order to remove the mismatch and thus eliminate the common boundary between them. Microstructures presented in this study and the observed explosive grain growth suggest that such a mechanism might be operative in the alloy. However, the validity of the subgrain coalescence mechanism has been questioned by several investigators, particularly with regard to the kinetics of the rotation process. The kinetics of grain rotation in alloy 718 cannot be computed unambiguously because of the uncertainties associated with the parameters such as self-diffusion coefficient and dislocation jog density, used in Li's kinetic equations.[30] The experimentally measured value of m for the steep portion of the growth curve was approximately 1, indicating a growth rate which was significantly higher than that for curvature-driven grain growth (m = 2 to 6). The growth rate appeared to decrease as the contribution from subgrain coalescence diminished and curvature-driven grain growth became the dominant mechanism.

There appeared to be a temporary retardation in the grain-growth kinetics, following the formation of a metastable grain-boundary liquid by the constitutional liquation of the carbides at this temperature (Figure 10).

However, the retardation is not as appreciable as the complete arrest in grain growth following the constitutional liquation of titanium sulfide inclusions in maraging steel.[7] A possible explanation for the observed difference in the grain-growth kinetics in the presence of metastable liquid in the two systems could be an inherent difference in the kinetics of wetting and spreading of the metastable liquid along the grain boundaries in the two alloy systems. However, a greater effect, which appeared to be related to the as-received microstructure of the 718 alloy used in this study, seems to be the elimination of subgrain boundaries by coalescence. Notice that grain growth by subgrain coalescence would not be retarded by the presence of liquid along the grain boundaries. In fact, continued grain growth in the presence of grain-boundary liquid by the coalescence of subgrains appeared to occur even at a peak temperature of 1227 °C.

2. *Grain growth at 1227 °C*

The grain-growth rate in this case does decrease monotonically as seen in Figure 10. Grain-growth data at 1227 °C were replotted with the quantity $(D^m - D_0^m)$ along the y-axis and the time t along the x-axis. The value of m was changed from an initial value of 0.5 to a final value of 6, in steps of 0.1. The best fit was obtained for a value of 3, with the best-fit line passing through the origin, as shown in Figure 11. Since the value of m is within the range of 2 to 6 observed for curvature-driven grain growth, the conclusion might be reached that the grain growth at 1227 °C in the presence of grain-boundary liquid was indeed curvature-driven. The kinetic equation is also in agreement with the generally accepted curvature-driven growth kinetics during the final stages of liquid-phase sintering where a linear relationship is observed between the grain size and $(\text{time})^{1/3}$.[31] However, several important differences have to be pointed out. First of all, the relationship in the case of liquid-phase sintering applies to the case of stable liquid. However, in the present study, most of the grain growth occurred in the presence of a liquid, a significant fraction of which was metastable. Figure 13 shows the reduction in the volume fraction of the liquid, during the time grain growth occurred. Also, for grain growth in the final stages of sintering, the stable liquid remains attached to the grain boundaries, either in the form of a continuous liquid if it wets the grain boundaries or as a discontinuous grain-boundary phase, which coarsens during grain growth. In either case, the linear relationship between grain size and $(\text{time})^{1/3}$ applies. However, in the present study, a significant fraction of the grain-boundary liquid film was converted to droplets of intragranular liquid by the sudden disappearance of many grain boundaries. Strong evidence of such occurrences is shown in Figures 4(a) through (d) and in Figure 5. Hence, the mechanism of grain growth at 1227 °C is not curvature-driven, and the linear relationship between grain size and $(\text{time})^{1/3}$ obtained in this study is rather fortuitously in agreement with curvature-driven grain growth in the presence of stable liquid. Finally, the reaction rate coefficient for grain growth given by the slope of the straight line in Figure 11 is 1623 μ^3/second, which is at least a couple of orders of magnitude higher than the values obtained in the literature for curvature-driven grain growth in the presence of grain-boundary liquid.[31]

The formation of a continuous film of grain-boundary liquid did result in a reduction in the grain-growth rate compared to that at 1200 °C (Figure 10). However, grain growth was not completely arrested as in 18Ni maraging steel[7] either. During the isothermal hold at this peak temperature, two major microstructural phenomena, LFM[24] and subgrain coalescence, were seen to occur simultaneously. The net result of these changes was an increase in the grain size as a function of isothermal hold.

3. *Liquid film migration*

The initial volume fraction of the liquid produced by the constitutional liquation of NbC, and possibly some supersolidus melting of the grain boundaries, was higher than the equilibrium volume fraction of liquid at 1227 °C (Figure 12). Hence, the system was initially not in chemical equilibrium. The equilibration of liquid volume fraction involves the diffusion of Nb atoms into the matrix at the S-L interface. This behavior causes a coherency strain in the matrix adjacent to the two S-L interfaces. The coherency strain energy at each interface is proportional to the coherency strain and the elastic modulus normal to the respective grain boundary. Because of an orientation mismatch across a grain boundary, the elastic moduli in the adjacent grains differ. A thermodynamic consideration of the equilibrium between the liquid and the stressed solid leads to a solute concentration gradient across the grain-boundary liquid film, which is known to cause the migration of the liquated boundaries.[16]

The microstructural features which support the occurrence of LFM are the formation of tortuous grain boundaries, the presence of circular grains (C), the formation of patches of liquid (P) at the triple points, and the formation of quadruple points (Q) shown in Figures 4(a) through (d). A schematic of the evolution of these microstructural features through LFM is shown in Figure 14. Since LFM makes the boundaries tortuous, the grain size as measured by the grain intercept method (N_L) should decrease with increasing LFM. The LFM can contribute to grain growth only if two migrating boundaries can collapse and form a single boundary; however, it is more likely that such a migration would lead to a quadruple point, as shown schematically in Figure 14. The boundary marked "T" in Figure 4b has a grain-boundary film which is much thicker than that in the neighboring boundaries, which seems to support the hypothesis that it formed by the collapse of two boundaries migrating toward each other. The effect of LFM on the grain size was not clear in the as-received alloy, since it occurred in the presence of subgrain coalescence, which contributes to grain growth.

4. *Subgrain coalescence*

It was mentioned earlier that subgrain coalescence occurred at a peak temperature of 1200 °C, which caused an exaggerated grain growth. The occurrence of such a process at 1227 °C could be clearly established by observing the liquation microstructures. Subgrain coalescence resulted in the elimination of some of the subgrain boundaries and the conversion of intergranular liquation into an intragranular liquation. Once the subgrain boundaries were eliminated, interfacial energy between the liquid and the matrix was minimized by the breaking up of the film into individual droplets. The formation of a row

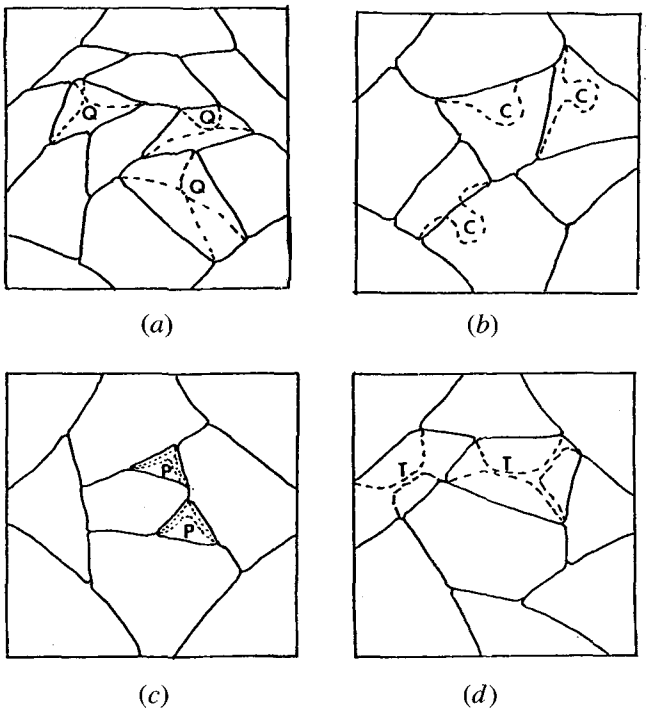

Fig. 14—Schematic of the progression of grain-boundary migration leading to the formation of (*a*) quadruple points, (*b*) circular grains, (*c*) pools of liquid at the triple points, and (*d*) variability in grain-boundary film thickness.

of droplets is shown in Figure 4. Figure 5 shows the breaking up of one such intragranular film into smaller streaks of intragranular liquid and finally into isolated droplets. Similar occurrences are also shown in Figure 4 (marked A, B, and C). Hence, it is clear that continued grain growth by subgrain coalescence occurred at a peak temperature of 1227 °C, which was not retarded by the presence of liquid along the subgrain boundaries.

The overall grain growth rate is determined by the combined effects of LFM and subgrain coalescence. The fact that a net grain growth was measured initially indicated that in the as-received alloy, subgrain coalescence was the dominant mechanism. With continued hold at 1227 °C, the contribution to grain growth by subgrain coalescence should decrease since the number of subgrains decreases. The LFM also should subside with isothermal hold since the system reaches chemical equilibrium with the elimination of the excess initial liquid. At this instant, the only growth mechanism is the curvature-driven grain growth which results in the reduction of the S-L interfacial area. However, since a continuous grain-boundary liquid is present, grain growth can occur only through diffusional transport of atoms across the film from a shrinking grain to a growing grain. Since the kinetics of this process is much slower compared to that of LFM and subgrain coalescence, it appears as if the grain size stabilizes to a limiting value in the time scales used in this study. At a peak temperature of 1200 °C where grain-boundary liquation was insignificant and could be completely eliminated by the isothermal hold, the grain-boundary carbides acted as obstacles to grain growth. At a peak temperature of 1227 °C, the obstacle to grain growth was the equilibrium liquid which remained on the grain boundaries after prolonged isothermal hold. The limiting grain size at 1227 °C was lower than at 1200 °C because of the greater volume fraction of grain-boundary liquid at 1227 °C than the intergranular carbides at 1200 °C.

B. *Homogenized and Aged Alloy*

1. *Grain growth at 1200 °C*

The rapid grain growth seen in the as-received alloy, following dissolution of δ, was absent in the homogenized and aged alloy (A). This could be primarily due to the elimination of the transient grain growth step involving subgrain coalescence during the prior homogenization heat treatment. The grain size of the homogenized and aged alloy (A) heated to a peak temperature of 1200 °C and quenched without isothermal hold was about 50 μ, while that of the as-received alloy after the rapid initial grain growth (isothermal hold of 8.4 seconds at 1200 °C) was about 58 μ. Hence, it is clear that most of the unstable grain growth which occurred in the as-received alloy during the isothermal hold at 1200 °C had already occurred during the homogenization and aging step prior to the isothermal hold at 1200 °C. Evidence of grain growth through subgrain coalescence during the homogenization heat treatment is shown in Figure 2, where disappearance of grain boundaries is indicated at the locations marked by arrows. Under these conditions, there was an arrest in the grain growth at 1200 °C, which appeared to be due to the presence of a grain-boundary liquid.[23] However, the formation of this grain-boundary liquid appeared to precede carbide liquation. Since the grain-boundary liquid film appeared to be extremely thin, it apparently wetted the grain boundaries completely. The liquid produced by the delayed, subsolidus liquation of the carbides also appeared to wet the boundaries. Grain growth appeared to resume immediately after the initial liquid was eliminated by a combination of diffusion and LFM. However, the extent of grain-boundary liquation was not significant enough to cause excessive LFM and significantly affect the grain size during the isothermal hold.

While grain-boundary liquation completely arrested grain growth in the homogenized and aged alloy at a peak temperature of 1200 °C, the as-received alloy showed an extremely high grain growth rate in spite of the grain-boundary liquation, which resulted in the elimination of the liquated boundaries and the conversion of grain-boundary liquid into droplets of intragranular liquid. Since the formation of liquation cracks depends upon the stability of the intergranular liquid, conversion of this liquid into an intragranular liquid should result in a decrease in the liquation cracking susceptibility of the alloy. It is very significant that liquation cracking in alloy 718 was considerably reduced by incorporating some cold work to the alloy prior to welding.[32] It was shown that the recrystallization of the HAZ grains during the weld thermal cycle prevented liquation cracking.[32] The present study tends to support such a hypothesis.

2. *Grain growth at 1227 °C*

The grain size as a function of isothermal hold in this case is entirely controlled by the kinetics of grain-boundary

migration. The migration at this temperature is apparently due to a supersolidus melting of the matrix which initiated at the grain boundaries and the subsequent depletion of niobium in the matrix at the S-L interface. A similar migration phenomenon has been recently observed by Muschik *et al.*[33] in the Cu-In system. Since chemical equilibrium involves the homogenization of the matrix composition to the niobium-depleted composition at the S-L interface, the excess solute should partition to the liquid and the volume fraction of the liquid should increase as a result of migration. The backscattered electron (BSE) image of a migrated grain boundary at this peak temperature (Figure 8) does not show the niobium enrichment behind the migrating boundary reported for a peak temperature of 1200 °C.[24] The BSE image does seem to indicate a niobium depletion (dark contrast on the concave side of the boundary), which is consistent with the supersolidus liquation hypothesis. Extensive migration results in the formation of tortuous grain boundaries and loops (L) shown in Figure 7. Since the initially straight grain boundaries become extremely curved, the N_L values increase as a function of isothermal hold, which causes an apparent decrease in the grain size. However, the formation of several small grains at the prior grain boundaries shows that nucleation of grains might be taking place during the migration process.

At first glance, it might seem that the isothermal hold at a peak temperature of 1227 °C produced opposing trends as far as grain growth was concerned. While grain growth was observed for the as-received alloy, a grain refinement was observed for the homogenized and aged alloy. However, in the as-received alloy, subgrain coalescence was the dominant mechanism which resulted in a net grain growth, while in the homogenized and aged alloys there was no subgrain coalescence. Liquid film migration was the dominant mechanism which resulted in an overall decrease in the grain size.

C. *Liquid Film Migration and Grain Refinement*

Figure 9 shows the microstructure at various locations along the gage length of a Gleeble sample, whose center was heated to a peak temperature of 1235 °C and quenched immediately after reaching the peak temperature. The sample was subjected to a homogenization heat treatment at 1093 °C for 100 seconds in the Gleeble prior to thermal cycling. The presence of a longitudinal temperature gradient in the sample enabled the observation of microstructures corresponding to different peak temperatures. The center of the Gleeble sample where the peak temperature was 1235 °C, corresponds to the extreme right location in Figure 9. The peak temperature progressively increases from left to right. The extreme left represents the location where liquation of the carbides just begins, as evidenced by the formation of a liquated region around the carbides. Notice that the grain boundaries in this region begin to show the reversed curvatures characteristic of LFM. There is a progressive decrease in the grain size as the peak temperature increases. The microstructures also show a progressive increase in the extent of liquid film migration, as evidenced by the formation of internal loops identical to those shown in Figure 7.

In the case of 18Ni maraging steel,[7] the grain refinement in HAZ regions close to the fusion line was attributed to the pinning of the grain boundaries by the metastable liquid produced by the constitutional liquation of the titanium sulfide inclusions in the steel. However, in the case of alloy 718, the grain refinement appears to be a consequence of the progressively increasing extent of grain-boundary migration in the HAZ close to the fusion line. Such a migration has not been reported in the supersolidus region of the HAZ in 18Ni maraging steel.

D. *Significance to Modeling of Liquation Cracking*

The interaction between the grain boundaries and metastable liquid can vary widely from one system to another even for comparable microstructures. While a complete arrest of grain growth was observed in the 18Ni maraging steel, the grain boundaries in alloy 718 migrated extensively in the presence of grain-boundary liquid. Differences exist between alloy systems relative to the kinetics of spreading and wetting of the metastable liquid along the grain boundaries, the temperature range over which subsolidus liquation occurs and the potential for LFM. Even within an alloy system, such as 718, the interaction between metastable liquid and grain boundaries could vary widely, depending upon the initial microstructure and thermal history of the alloy. In alloy systems where no LFM occurs, the solidification of the grain-boundary liquid can be modeled assuming a stationary boundary. However, in alloy systems where significant migration of the liquated boundaries occur during the heating and as well as the cooling cycle, the contribution to the formation and solidification of grain-boundary liquid from LFM should also be considered. Migration results in an increase in the grain-boundary surface area and either an increase or decrease of the grain-boundary film thickness, depending upon whether the migration occurs at the supersolidus or subsolidus temperature range.

The occurrence of grain growth through subgrain coalescence has remained a controversial subject over the years. The kinetics of coalescence cannot be computed unambiguously for a complicated alloy system such as 718. However, there is strong microstructural evidence for grain coalescence in the alloy. The obvious effect of such a mechanism is to convert an intergranular film of liquid into an intragranular liquid, which makes the microstructure more resistant to liquation cracking.

V. CONCLUSIONS

1. The extent to which subsolidus liquation could arrest grain growth in the subsolidus HAZ of alloy 718 was found to depend on the thermal history of the alloy.
2. The unpinning of grain boundaries by dissolving δ precipitates in the as-received alloy resulted in an explosive grain growth at a peak temperature of 1200 °C. The kinetics of grain growth was appreciably greater than that of a curvature-driven grain growth phenomenon.
3. Isothermal liquation microstructures at the above peak temperature indicated that grain growth occurred by

the coalescence of subgrains produced in the as-received alloy during hot-working.

4. In the homogenized and aged alloy, there was an arrest of grain growth upon isothermally holding at a peak temperature of 1200 °C.
5. The extent of LFM at 1200 °C was not significant enough to affect the grain size as function of isothermal hold for the homogenized and aged alloy.
6. At the supersolidus temperature of 1227 °C, grain growth continued to occur by the subgrain coalescence mechanism in the as-received alloy. The role of LFM was to drive the system toward chemical equilibrium by eliminating the excess liquid and the concentration gradients produced by the liquation of carbides and δ phase. The LFM resulted in the formation of several interesting microstructural features in the as-received alloy.
7. In the homogenized and aged alloy, the grain size was controlled essentially by the extent of LFM, which resulted in a decrease of grain size as a function of isothermal hold. A similar grain refinement was observed in the supersolidus HAZ of the homogenized alloy as a function of peak temperature.
8. Modeling of solidification of the grain-boundary liquid could be complicated not only by the occurrence of LFM, but also by microstructural processes such as subgrain coalescence which could convert intergranular liquation into an intragranular liquation.

ACKNOWLEDGMENT

The authors would like to acknowledge the financial support given to this research by the National Science Foundation under Grant No. DMR-8807915.

REFERENCES

1. J.J. Pepe and W.F. Savage: *Welding Journal*, 1967, vol. 46, pp. 411-s-422-s.
2. W.A. Owczarski, D.S. Duvall, and C.P. Sullivan: *Welding Journal*, 1967, vol. 46, pp. 423-s-432-s.
3. B. Weiss, G.E. Grotke, and R. Stickler: *Welding Journal*, 1970, vol. 49, pp. 471-s-487-s.
4. J.A. Brooks: *Welding Journal*, 1974, vol. 53, pp. 517-s-523-s.
5. W.A. Baeslack III, S.J. Savage, and F. Froes: *Journal of Materials Science Letters*, 1986, pp. 935-39.
6. A.D. Romig, Jr., J.C. Lippold, and M.J. Cieslak: *Metall. Trans. A*, 1988, vol. 19A, pp. 35-50.
7. J.J. Pepe and W.F. Savage: *Welding Journal*, 1970, vol. 49, pp. 545-s-553-s.
8. B. Radhakrishnan and R.G. Thompson: *Metall. Trans. A*, 1992, vol. 23A, pp. 1783-99.
9. I.A. Aksay, C.E. Hoge, and J.A. Pask: *J. Phys. Chem.*, 1974, vol. 78, pp. 1178-83.
10. T.P. Isaac, M. Dollar, and T.B. Massalski: *Metall. Trans. A*, 1988, pp. 675-86.
11. D. McLean: *Grain Boundaries in Metals*, Oxford University Press, London, 1957.
12. E.D. Hondros and M.P. Seah: *Intl. Metals Rev.*, 1977, vol. 22, pp. 262-301.
13. J.C. Lippold: *Welding Journal*, Jan. 1983, vol. 62, pp. 1s-11s.
14. D.N. Yoon: *Annu. Rev. Mater. Sci.*, vol. 19, 1989, pp. 43-58.
15. C.A. Handwerker: in *Diffusion Phenomena in Thin Films and Microelectronic Materials*, D. Gupta and P.S. Ho, eds., Noyes Publications, New Jersey, U.S.A.
16. M. Hillert: *Scripta Metall.*, 1983, vol. 17, pp. 237-40.
17. R.G. Thompson and S. Genculu: *Welding Journal*, Dec. 1983, vol. 62 (12), pp. 337s-345s.
18. W.A. Baeslack III and D.E. Nelson: *Metallography*, 1986, vol. 19, pp. 371-79.
19. P.J. Valdez and J.B. Steinman: *Effect of Minor Elements on the Weldability of High-nickel Alloys*, Welding Research Council, New York, 1969, pp. 93-120.
20. E.G. Thompson: *Welding Journal*, Feb. 1969, vol. 48 (2), pp. 70s-79s.
21. T.J. Kelly: Trends in Welding Research, ASM, 1986.
22. B. Radhakrishnan and R.G. Thompson: *Metall. Trans. A*, 1991, vol. 22A, pp. 887-902.
23. B. Radhakrishnan and R.G. Thompson: *Metall. Trans. A*, 1993, vol. 24A, pp. 1409-22.
24. B. Radhakrishnan and R.G. Thompson: *Scripta Metall.* 1990, vol. 24, pp. 537-42.
25. J.G. Byrne: *Recovery, Recrystallization and Grain Growth*, Macmillan Co., New York, 1965.
26. G. Muralidharan: Masters Thesis, University of Alabama at Birmingham, 1988.
27. D.J. Srolovitz, G.S. Grest, and M.P. Anderson: *Acta Metall.*, 1985, vol. 33, pp. 2233-47.
28. N.A. Wilkinson: in *Superalloy 718: Metallurgy and Applications*, E.A. Loria, ed., TMS, Warrendale, PA, 1989, pp. 119-33.
29. J.L. Burger, R.R. Biederman, and W.H. Couts: in *Superalloy 718: Metallurgy and Applications*, E.A. Loria, ed., TMS, Warrendale, PA, 1989, pp. 207-17.
30. J.C.M. Li: *J. Appl. Phys.*, 1962, vol. 33, p. 2958.
31. R.M. German: *Liquid Phase Sintering*, Plenum Press, New York, 1985, pp. 133-43.
32. C. Boucher, D. Varela, M. Dadian, and H. Granjon: *Revue de Metallurgie*, Dec. 1976, pp. 817-31.
33. T. Muschik, W.A. Kaysser, and T. Hehenkamp: *Acta Metall.*, 1989, vol. 37, pp. 603-13.